Reaction Kinetics, Mechanisms and Catalysis (2023) 136:367–379
https://doi.org/10.1007/s11144-023-02357-4

The effect of nanocrystalline TiO_2 on structure and catalytic activity of CuO–ZnO in combined methanol reforming

F. Pinzari[1]

Received: 1 December 2022 / Accepted: 19 January 2023 / Published online: 1 February 2023

Abstract

CuO–ZnO (CZ) and CuO–ZnO/TiO_2 (CZT) catalysts have been prepared by co-precipitation, characterized by X-ray diffraction, surface area measurements and chemical analysis and tested in the combined methanol reforming reaction. Catalytic tests have been performed in the temperature range 200–400 °C with a GHSV = 55.000 h^{-1}, after H_2 reducing pretreatment at 250 °C or 450 °C. It is shown that nanocrystalline TiO_2 influences the CuO–ZnO nanosized structure, reducibility and reactivity. TiO_2 slightly increases ZnO crystallite size of the fresh catalyst. Moreover, it causes the CuO chemical reduction to nanosized Cu_2O on exhaust catalyst pretreated in hydrogen at 250 °C, this improves the reaction with higher methanol conversion and hydrogen production. On the contrary, TiO_2 reduces CuO to submicron Cu^0 and greatly increases ZnO crystallite size on the exhaust catalyst pretreated in hydrogen at 450 °C, this treatment weakens the reaction, with lower methanol conversion and hydrogen production. In both cases, nanocrystalline TiO_2 presence is able to decrease the CO formation: independently of the hydrogen pretreatment temperature. This ability of the nanocrystalline TiO_2 is ascribed to the presence of the oxygen vacancies, which act as electron donors that contribute to hinder CO_2 and H_2 surface adsorption for steric, electrostatic and probabilistic factors.

Keywords CuO · ZnO · TiO_2 · Combined methanol steam reforming · Crystallite size · Nano sized

Introduction

Methanol steam reforming (MSR) is a suitable reaction to produce hydrogen for PEM fuel cell.

✉ F. Pinzari
fulvia.pinzari@cnr.it

[1] CNR – ISPC, Via Salaria, Km 29.300, Monterotondo Scalo, Rome, Italy

$$CH_3OH + H_2O \rightarrow 3H_2 + CO_2. \quad (1)$$

It is an endothermic reaction ($\Delta H = +49.4$ kJ mol^{-1}) and thus requires high temperatures, moreover carbon monoxide, due to side reaction [1], can be formed as a by-product, both factors can affect the fuel cell performances up to ruin it [2]. Velu et al. [3] indicated that a suitable amount of oxygen could reduce CO formation and contribute to decrease the reaction temperature because the methanol oxidation (MO) reaction takes place.

$$CH_3OH + \frac{1}{2}O_2 \rightarrow 2H_2 + CO_2. \quad (2)$$

This is an exothermic reaction ($\Delta H = -192.2$ kJ mol^{-1}), so it supplies heat and lowers the overall reaction temperature, moreover the presence of O_2 helps to decrease the CO content in the outgoing gas mixture; MSR produces three hydrogen molecules for each methanol molecule, while MO only two. A combination of MSR and MO, the so called oxidative methanol reforming or combined methanol reforming (CMR), has been proven to be energetically favorable and helpful to minimize CO production [2].

$$CH_3OH + \alpha H_2O + \beta\frac{1}{2}O_2 \rightarrow (2+\alpha)H_2 + CO_2, \quad (3)$$

With $(\alpha + \beta) = 1$.

CuO–ZnO are catalysts commonly used for methanol synthesis from CO_2 [4].

$$3H_2 + CO_2 \rightarrow CH_3OH + H_2O. \quad (4)$$

As Eq. 4 is the reverse of Eq. 1, Amphlett et al. [5, 6] studied CuO–ZnO catalysts in methanol steam reforming in the temperature range 150–370 °C, using W/F = 300–1400 kg s mol^{-1}, finding 80% methanol conversion. Breen et al. [1] studied the system CuO–ZnO/ZrO_2/Al_2O_3, finding a complete methanol conversion at 300 °C with W/F = 0.004 g min cm^{-3}. Zhang et al. [7] studied the effect of ZrO_2 and CeO_2 on the CuO-ZnO catalysts in methanol steam reforming, and found that ZrO_2 increased Cu dispersion with a consequent increase of methanol conversion and CeO_2 could enhance oxygen storage with a decrease in CO production. Chang et al. [8] studied the effect of Al_2O_3, CeO_2 and ZrO_2 on catalytic performances of CuO–ZnO and found that all of them enhanced CuO and ZnO dispersion, Al_2O_3 decreased catalyst reducibility and weakened the reaction but gave mechanical strength to the catalyst, CeO_2 increased catalyst reducibility but weakened the reaction and ZrO_2 improved catalyst reducibility and promoted the reaction.

Our previous study [9, 10] focused on the system ZnO/TiO_2, showed that it is active in methanol steam reforming with a complete reaction at T = 400 °C and GHSV (CH_3OH) = 5 * 10^4 h^{-1}. The activity of the system was attributed to the ZnO phase, TiO_2 was useful to enhance surface area and to decrease CO formation, the best results were found when $\chi_{Zn} = 0.05$, segregation of ZnO was evident with higher Zn content, which caused the decrease in surface area and subsequent inhibition of the reaction. Later other authors have reported on the activity of Zn/TiO_2

catalysts in the methanol steam reforming. Griboski et al. [11] ascribe the system reactivity of the system Zn/TiO_2 to the zinc titanate presence and Deshmane et al. [12] relate the reactivity to the TiO_2 dispersion, no consideration about zinc textural properties are reported and there is no ZnO evidence. Eaimsumang et al. [13] studied the effect of the morphology and crystalline phases of pristine TiO_2 on oxidative steam reforming of methanol, showing that rutile or mixed phases are more active than anatase.

Xiao et al. [14, 15] studied the effects of TiO_2 on CuO-ZnO in methanol synthesis, and found that amorphous TiO_2 decreases CuO and ZnO crystallite size, changes CuO reducibility with a maximum of Cu^0 surface area when $TiO_2 = 13\%$ mol, which promoted highest CO_2 conversion. Zhang et al. [16, 17] studied the effects of TiO_2 on $CuO\text{-}ZnO/Al_2O_3$ in methanol synthesis and found that a little amount of amorphous TiO_2 improves CuO dispersion, allowing a better adsorption/activation of H_2 and CO_2 and thus increases the reaction. Khani et al. [18] studied the hybrid thermo-photo catalytic reforming of methanol by $CuZn/TiO_2$ (ZnO is supposed nanocrystalline or amorphous), and found a conversion of 35% and 63% at 150 and 200 °C, respectively, with a WHSV of 8.5 h^{-1} and $H_2O/CH_3OH = 1$. D. V. Andreev et al. [19] studied the system $CuZn/TiO_2$ in methanol steam reforming with a WHSV = 4.43 h^{-1} and found a conversion of 40%, 90% and 100% at T = 375, 400 and 450 °C, in this case, Zn forms Zn_2TiO_4.

ZnO and TiO_2 are widely studied in the literature because they are used as photocatalysts [20] and dye sensitized solar cell [21]. CuO, ZnO and TiO_2 are commonly used as catalysts in different reaction [22], particularly in organic synthesis [23], moreover they have biocidal properties and this makes them useful in water decontamination [24] and stone protection in the field of cultural heritage [25, 26].

In this paper, we report preliminary results on the effect introduced by nanocrystalline TiO_2 on CuO-ZnO catalyst, focusing our attention on structure, reducibility and catalytic performance in CMR, after hydrogen reducing pretreatment performed at 250 or 450 °C.

Experimental

CuO–ZnO (CZ) catalyst was prepared by co-precipitation of carbonates in a similar way to Okamoto et al. [27]. Na_2CO_3 (Merck), zinc nitrate hexahydrate (Aldrich) and Copper (II) nitrate hemi (pentahydrate) (Aldrich) were used as starting reagents. A water solution containing zinc nitrate (0.1 M) and copper (II) nitrate (0.04 M) was prepared under magnetic stirring and kept in N_2 bubbling, then a Na_2CO_3 water solution (0.4 M) was added dropwise, then the temperature was raised to 80 °C for 3 h. At the end the pH of the solution was 9, the precipitate was decanted overnight, washed with distilled water to eliminate all sodium, filtered, dried at 90 °C for 12 h and calcined at 350 °C for 3 h. $CuO–ZnO/TiO_2$ (CZT) catalyst was prepared as CZ, TiO_2 (Aldrich, anatase) was added in the water solution containing copper and zinc nitrate.

CMR reactions was studied. Catalytic tests were performed in a fixed bed quartz reactor with an inner diameter of 1 cm. A suitable amount of catalyst was diluted 1/10 in sieved α-Al_2O_3, and then put into the reactor that had already been filled up to 2 cm with 1 mm diameter SiO_2 balls. The catalysts were pretreated in (10%) H_2/He mixture at 250 °C or 450 °C for 2 h, the temperature was raised at 5 °C min^{-1}. Catalytic tests were performed in the range of temperature 200–400 °C. A solution of methanol in water was introduced into the reactor by a syringe pump (Sage Instruments model 341 A), O_2 and He flows were regulated by flowmeters. The reaction condition settings are summarized in Table 1. A blank test was performed with a reactor containing only SiO_2 balls and α-Al_2O_3.

The temperature of the catalysis line from the reactor outlet to the chromatograph automatic sampling area was kept at 120 °C, so that CH_3OH and H_2O vapors were transported by the vector gas and analyzed together with other gas components. The reaction products were analyzed by a Carlo Erba 4300 GC, equipped with a Hayesept D column, products were detected by a thermal conductivity detector.

In the following CZ(T) refers to the as calcined catalysts, CZ(T)250(or 450) refers to the catalyst exhaust, 250 or 450 indicate the hydrogen pretreatment temperature.

A Philips PW 100 diffractometer with a Ni-filtered Cu K_α ($\lambda_{Cu} = 1.54$ Å) radiation was used to record powder X-ray diffraction patterns. Spectra were collected on fresh and exhaust catalysts. Crystallite sizes (d) were calculated by the Debye Scherrers equation:

$$d = K\lambda/\beta\cos\theta,$$

Here k is a constant (0.9), λ is X-ray wavelength, β is the FWHM diffraction peak and θ is the diffraction angle.

A Varian Spectra A-30 Instrument atomic absorption was used to determine elemental composition. Surface area of catalysts were calculated by the BET

Table 1 Combined methanol reforming reaction conditions

Gas	Composition (%)	$\frac{W}{F}$[a]		WHSV[b]	GHSV[c]
	(n or V)	(g min cc^{-1})	(kg s mol^{-1})	(h^{-1})	(h^{-1})
CH_3OH	16.9	0.0059	8.0	14.5	55.000
H_2O	18.5	0.0054	7.3	8.9	60.000
O_2	2.0	0.050	67.2	0.9	6.000
He (vector gas)	62.6	0.0016	2.1	3.3	203.000
tot	100	0.001	1.3	27.6	324.000

[a] $\frac{W}{F} = \frac{W_{cat}}{f_{gas}}$

[b] $WHSV = \frac{M^h_{gas}}{M_{cat}}$

[c] $GHSV = \frac{V^h_{gas}}{V_{cat}}$

GHSV has been calculated assuming a mean density value = 5.4 g cc^{-1}

isotherm of N_2 adsorption by a Micromeritics ASAP 2010 analyzer after having degassed the catalyst in vacuum at 170 °C.

Results and discussion

Catalysts have been prepared in such a way to get the same ZnO/CuO ratio, with the aim to study the effect introduced by the nanocrystalline TiO_2 presence. We report chemical composition and surface area of fresh CZ and CZT catalysts in Table 2. The nanocrystalline TiO_2 presence slightly increases surface area.

CH_3OH, H_2O, CO, CO_2 and H_2 were found during catalytic tests, no other species were detected. CH_3OH conversion, CO selectivity and H_2 yield were calculated as follows:

$$\text{CH}_3\text{OH conversion} = \frac{[\text{CO}] + [\text{CO}_2]}{[\text{CO}] + [\text{CO}_2] + [\text{CH}_3\text{OH}]},$$

$$\text{CO selectivity} = \frac{[\text{CO}]}{[\text{CO}] + [\text{CO}_2]},$$

$$\text{H}_2\text{ yield} = \frac{[\text{H}_2]}{[\text{CO}] + [\text{CO}_2] + [\text{CH}_3\text{OH}]}.$$

Catalyst performances obtained in CMR reaction after hydrogen pretreatment at 450 °C are compared for ZC and ZCT in Fig. 1.

Methanol conversions (Fig. 1a) and hydrogen yields (Fig. 1b) as a function of the temperature have the classical sigmoidal shape. Nanocrystalline TiO_2 presence in the catalyst decreases both of them in the fast increasing part of the sigmoid (T = 250 and 300 °C), however it allows to get a slightly higher value of hydrogen yield when the reaction reaches completeness. CO selectivity increases with the temperature (Fig. 1c) and with the methanol conversion (Fig. 1d) for both catalysts, it is evident that the nanocrystalline TiO_2 presence decreases the CO production.

Catalyst performances of ZC and ZCT after hydrogen pretreatment at 250 °C are compared in Fig. 2. Also in this case methanol conversion (Fig. 2a) and hydrogen yield (Fig. 2b) values have a sigmoidal shape. TiO_2 presence decreases the reaction at lower temperature and increases the reaction at higher temperature,

Table 2 Chemical composition and surface area of the catalysts

Catalyst	TiO_2 (% mol)	ZnO (% mol)	CuO (% mol)	ZnO/CuO	S. A (m^2g^{-1})
CZ	–	74	26	2.8	80
CZT	36	47	17	2.8	105

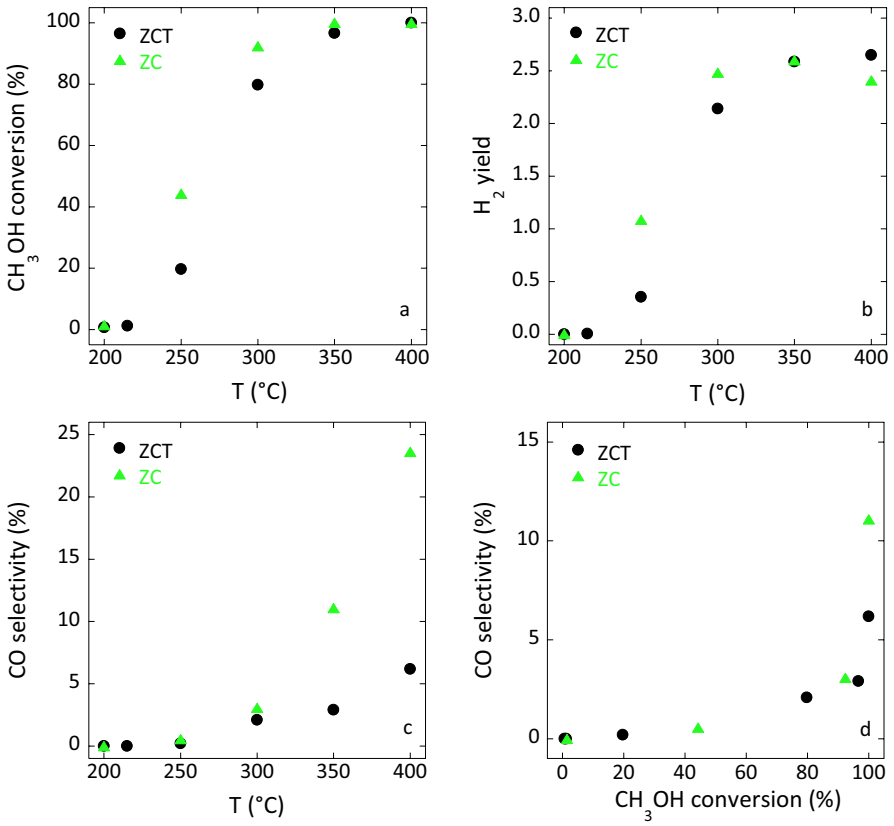

Fig. 1 Catalyst performances obtained for ZCT (black circles) and ZC (green triangles) after hydrogen pretreatment at 450 °C in H_2/He (10%) for CMR. Reaction conditions: $G_{CH3OH}HSV = 55.000\ h^{-1}$, $O_2 = 2.0\%$, $H_2O = 18.5\%$, $CH_3OH = 16.9\%$, $He = 62.6\%$. (Color figure online)

so the completeness of the reaction is reached at a lower temperature. Hydrogen yield trends (Fig. 2b) seem to reflect methanol conversions trends. CO selectivity values have again an increasing trend as a function of the temperature (Fig. 2c) and the methanol conversion (Fig. 2d). The nanocrystalline TiO_2 is useful to decreases CO selectivity as a function methanol conversion when methanol conversion is higher than 50%.

Resuming nanocrystalline TiO_2 presence affects CuO–ZnO catalytic activity, it decreases the reactivity when the hydrogen reducing pretreatment is performed at 450 °C and increases the reactivity when the hydrogen reducing pretreatment is performed at 250 °C. Lower CO production is observed with the catalyst containing nanocrystalline TiO_2 independently of the temperature of the pretreatment.

The methanol conversion and the hydrogen yield obtained after the catalytic tests after the two different hydrogen pretreatment temperatures are compared in Fig. 3 for ZCT (Fig. 3a) and ZC (Fig. 3b). It can be easily seen that the hydrogen pretreatment temperature affects the methanol conversion and hydrogen yield of ZCT, but

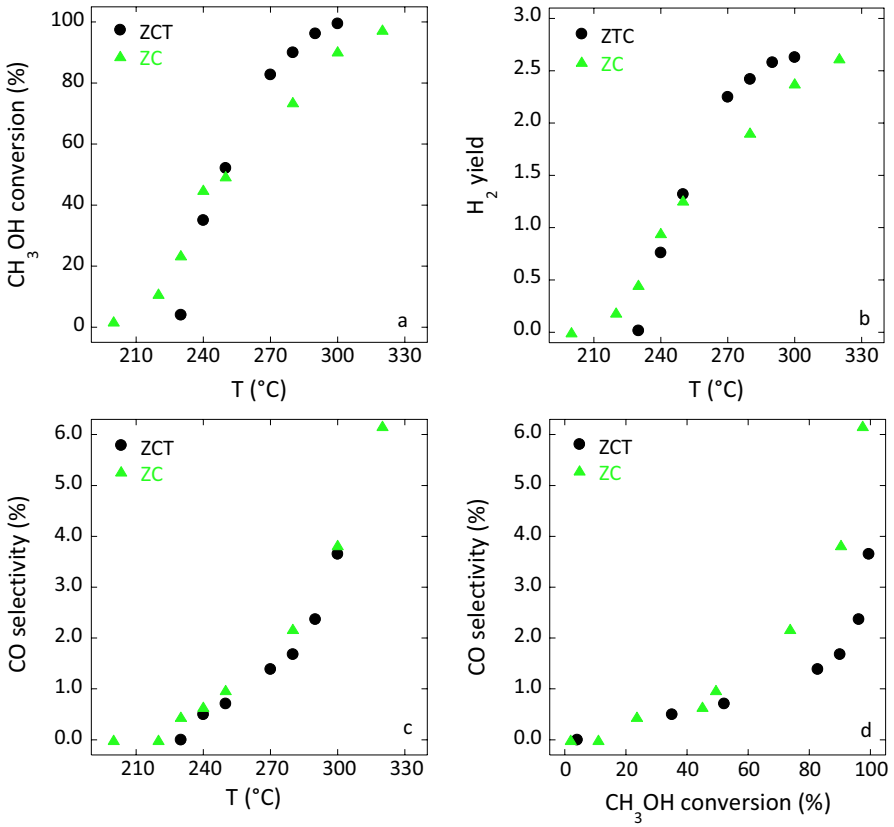

Fig. 2 Catalyst performances obtained for ZCT (black circles) and ZC (green triangles) pretreated in hydrogen at 250 °C for CMR. Reaction conditions: $G_{CH3OH}HSV = 55.000\ h^{-1}$, $O_2 = 2.0\%$, $H_2O = 18.5\%$, $CH_3OH = 16.9\%$, $He = 62.6\%$. (Color figure online)

does not change those of ZC. It is now clear that TiO_2 makes the catalyst performance more sensible to the temperature of the hydrogen pretreatment.

Investigation about differences caused by the hydrogen pretreatment temperature have been studied by X-ray diffraction, which has been performed on the fresh and exhaust catalysts. The diffractograms are reported in Fig. 4, TiO_2 (Aldrich) anatase diffraction pattern (T) is also reported for a comparison. Fig. 4a displays diffraction patterns of fresh ZC, ZCT and T. ZC and ZCT clearly present ZnO in wurtzite phase (JCPDS Card No. 36-1451) [28] with (100), (002) and (101) reflections at $2\theta = 31.7$, 34.5 and 36.2. Anatase phase (JCPDS: No 21-1272) [29] is the only component of T and is present in ZCT, showing its highest reflection (101) at $2\theta = 25.3$, secondary reflections are also present, as labelled in Fig. 4a. Fig. 4b shows ZC and ZCT diffractograms in the region $28° \leq 2\theta \leq 42°$, recorded as a result of a greater number of acquisitions, to get a higher signal/

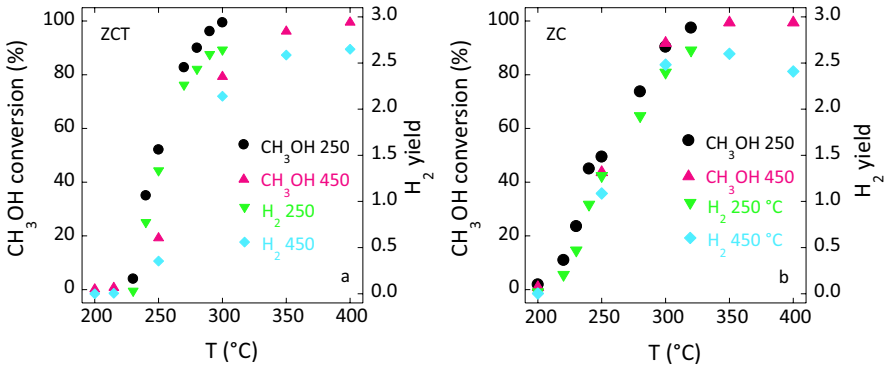

Fig. 3 influence of the hydrogen temperature pretreatment on methanol conversion and hydrogen yield of ZCT (**a**) and ZC (**b**). Black circles = CH_3OH conversion after H_2 pretreatment at 250 °C, pink triangles CH_3OH conversion after H_2 pretreatment at 450 °C, green triangle upside = hydrogen yield after H_2 pretreatment at 250 °C, blue rhombus = hydrogen yield after H_2 pretreatment at 450 °C. Reaction conditions: $G_{CH3OH}HSV = 55.000\ h^{-1}$, $O_2 = 2.0\%$, $H_2O = 18.5\%$, $CH_3OH = 16.9\%$, $He = 62.6\%$. (Color figure online)

noise ratio. Moreover, since (111) CuO diffraction peak almost overlaps the (004) anatase diffraction peak, a suitable subtraction of the TiO_2 spectra has been performed. CuO in tenorite phase (111) reflection at $2\theta = 38.8$ (JCPDS card no. 45-0937) [30] is visible with a very low intensity for both catalysts.

X-ray diffraction patterns of exhaust ZC and ZCT are reported in Figs. 4c, d, respectively, compared with those of the fresh ones. Wurtzite is the dominant phase in ZC450 catalyst (Fig. 4c), tenorite phase is present, both phases show narrower peaks than CZ diffractogram, meaning that the hydrogen pretreatment and catalytic tests promote an increase in crystallite size. Anatase and wurtzite are dominant phases in all ZCT (250 or 450) diffractograms (Fig. 4d), tenorite phase is still present with low intensity. Cu_2O in cuprite phase (JCPDF no. 78-2076) [31] is visible in ZCT250 by (200) diffraction peak at $2\theta = 42.3$, the main Cu_2O diffraction peak (111) at $2\theta = 36.5$ is hidden by the more intense wurtzite (101) peak in the same region. Cu^0 (JCPDF no. 85-1326) [31] formation in CZT450 is pointed out by (111) and (200) diffraction peaks at $2\theta = 43.4°$ and 50.4°, respectively.

In Table 3, we report the crystallite size of all phases as calculated by Debye Scherrer's equation. X-ray analysis reveals the nanocrystalline structure of ZC and ZCT fresh catalysts; wurtzite and tenorite phase crystallite sizes are only slightly increased by the nanocrystalline TiO_2 presence. Catalytic tests and hydrogen pretreatments cause complex changes in the structure. Comparing ZC with ZC450 we can observe that the H_2 reducing pretreatment and catalytic test induce a little increase in crystallite size on both wurtzite and tenorite, but a good dispersion is still present. Viceversa comparing ZCT with ZCT250 and ZCT 450 a higher increase in ZnO crystallite size is observed, together with a gradual chemical reduction of CuO to Cu_2O and Cu^0. All ZCT250 phases are still well dispersed, it's not so in ZCT450, where the formation of submicron phases of ZnO and Cu^0 is found. Our experiments show that the nanocrystalline TiO_2 presence slightly increases ZnO and CuO

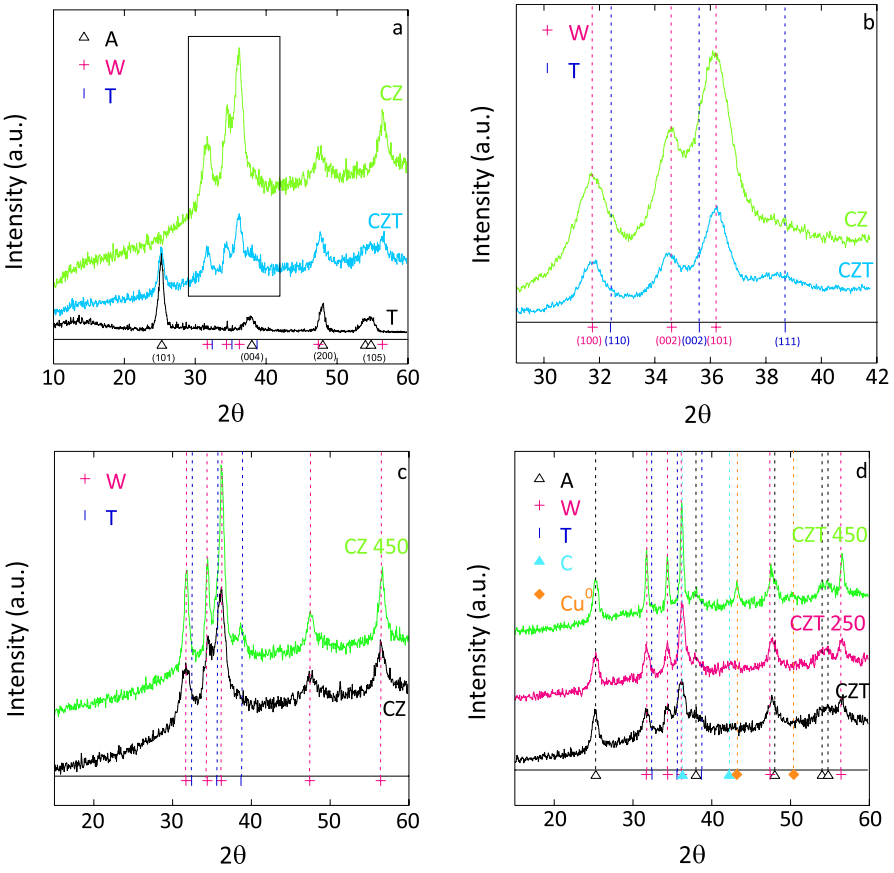

Fig. 4 X-ray diffraction pattern of ZC and ZCT catalysts (**a**, **b** inset enlarged) CZ 450 (**c**) and CZT 250 and CZT 450 (**d**). *A* anatase TiO_2, *W* wurtzite ZnO, *T* tenorite CuO, *C* cuprite Cu_2O

Table 3 Crystallite size (nm)

Catalyst	TiO_2	ZnO	CuO	Cu_2O	Cu^0
T	26	–	–	–	–
ZCT	32	26	4	–	–
ZCT 250	23	40	13	5	–
ZCT 450	32	158	11	–	80
ZC	–	13	2	–	–
ZC 450	–	53	13	–	–

crystallite size and makes CuO more reducible. This result is apparently in contrast with the literature [14, 32], where amorphous TiO_2, increased dispersion of ZnO and CuO and decreased CuO reducibility. Nanocrystalline TiO_2 has oxygen vacancies, which are as electron donors and form n-type levels, in amorphous TiO_2 n-type

level formation cannot be ensured. On the other hand, electron donors centers can interact with CuO and ZnO ionic structure, causing a lower dispersion and a higher reducibility of CuO.

We had shown that nanocrystalline TiO_2 presence enhanced the CRM reaction if the hydrogen pretreatment was carried out at T = 250 °C (Fig. 2), and decreased the reaction if the hydrogen pretreatment was carried out at T = 450 °C (Fig. 1). We had also shown that this variation was due to a change in the catalytic performance of ZCT induced by the different hydrogen pretreatment temperature, while ZC performance remained unchanged (Fig. 3). We can now deduce that a nanosized structure of CuO and ZnO is essential to get good catalytic performance, highest methanol conversion and hydrogen yield of ZCT250 are ascribed to the formation of nanosized and Cu_2O, while lowest methanol conversion and hydrogen yield of ZCT450 are ascribed to formation of submicron ZnO and Cu^0.

Moreover, since CZT250 and CZT450 produce less CO than CZ250 and CZ450 respectively, we attribute the ability to decrease CO formation to the nanocrystalline TiO_2 presence. It has been previously established [1, 33] that CO formation during methanol reforming reactions over CuO–ZnO catalysts is due the retro water gas shift reaction (r-WGS):

$$CO_2 + H_2 \rightarrow CO + H_2O. \quad (5)$$

Thus, a catalyst can facilitate this reaction if it is able to attract and adsorb the molecule of CO_2 or H_2. Both molecules have a linear shape; H_2 molecule has a net electric dipole moment of zero, thus its adsorption could be facilitate by a catalyst with no electric charge on the surface. The CO_2 molecule, with no net electric dipole, has a δ^- charge at the ends and a δ^+ charge in the center, because of steric/electric and probabilistic factors, its adsorption could be facilitated by the presence of positive charges, and be made more difficult by the presence of negative charges on the surface of the catalyst. It is still the presence of n-type levels on the nanocrystalline TiO_2 that will tend to impede the CO_2 adsorption and subsequently the r-WGS reaction, resulting in a final decrease of CO formation. These considerations are not in contrast with Zhang et al. [17], who attributed to TiO_2 the ability to facilitate the adsorption of H_2 and CO_2 in CZT catalysts, because TiO_2 was amorphous or highly dispersed, such as not to be detectable by X-ray diffraction. In that case, the presence of n-type levels could not be ensured as already explained.

Conclusions

In this work, we have shown that nanocrystalline TiO_2 affects CuO-ZnO structure and catalytic activity in CMR. Nanocrystalline TiO_2 causes a slight increase in ZnO (wurtzite) crystallite size and does not significantly change the size of CuO crystallites (tenorite) after calcination at 350 °C. Both wurtzite and tenorite phases are strongly influenced by nanocrystalline TiO_2 presence after catalytic tests: wurtzite phase undergoes an increase in crystallite size, this effect is moderate if the

hydrogen pretreatment is performed at 250 °C and is stronger the hydrogen pretreatment is performed at 450 °C, causing the formation of submicrometer crystallites. Tenorite phase undergoes a slight increase in crystallite size, resulting always nano sized and well dispersed. However, nanocrystalline TiO_2 presence makes tenorite more chemically reducible, which causes the formation of nanosized Cu_2O (cuprite) and submicron Cu^0 after catalytic tests performed after hydrogen pretreatment at 250 °C and 450 °C.

It has been shown that TiO_2 presence increases CuO–ZnO catalytic activity upon hydrogen pretreatment at 250 °C and decreases it upon pretreatment at 450 °C.

The best catalytic performances of the CZT250 are thus associated to the nano sized ZnO and well dispersed CuO and Cu_2O, the worst catalytic performances of CZT 450 are in turn associated to the loss of the nanocrystalline nature of the catalyst with the formation of submicron ZnO and Cu^0.

In the end, it has been proven that the nanocrystalline TiO_2 plays a clear role in limiting the production of CO, independently of the pretreatment temperature. This ability of nanocrystalline TiO_2 is ascribed to the presence of the oxygen vacancies, which act as electron donors, which contribute to hinder the CO_2 and H_2 surface adsorption, which is a necessary step to produce CO by r-WGS reaction.

Funding Open access funding provided by Consiglio Nazionale Delle Ricerche (CNR) within the CRUI-CARE Agreement.

Declarations

Conflict of interest The author has no financial interest to disclose.

References

1. Breen JP, Meunier FC, Ross JRH (1999) Mechanistic aspects of the steam reforming of methanol over a CuO/ZnO/ZrO2/Al2O3 catalyst. Chem Commun. https://doi.org/10.1039/A906393E
2. Song C (2002) Fuel processing for low-temperature and high-temperature fuel cells challenges, and opportunities for sustainable development in the 21st century. Catal Today 77:17–49. https://doi.org/10.1016/S0920-5861(02)00231-6
3. Velu S, Suzuki K, Osaki T (1999) Oxidative steam reforming of methanol over CuZnAl(Zr)-oxide catalysts; a new and efficient method for the production of CO-free hydrogen for fuel cells. Chem Commun. https://doi.org/10.1039/A907047H

4. Kotera Y, Oba M, Ogawa K, Shimomura K, Uchida LH (1976) The preparation of the catalysts for methanol synthesis and their characteristics. Stud Surf Sci Catal 1:589–599. https://doi.org/10.1016/S0167-2991(08)63982-8
5. Amphlett JC, Evans MJ, Mann RF, Weir RD (1985) Hydrogen production by the catalytic steam reforming of methanol. Part 2: kinetics of methanol decomposition using Girdler G66B catalyst. Can J Chem Eng 63:605–611. https://doi.org/10.1002/cjce.5450630412
6. Amphlett JC, Mann RF, McKnight C, Weir RD (1985) Production of a hydrogen-rich gas by steam reforming of methanol over copper oxide-zinc oxide catalysts. IECEC Proceedings, 772–780
7. Zhang L, Pan L, Ni C, Sun T, Zhao S, Wanga S, Wang A, Hu Y (2013) CeO2eZrO2-promoted CuO/ZnO catalyst for methanol steam reforming. Int J Hydrog Energy 38:4397–4406. https://doi.org/10.1016/j.ijhydene.2013.01.053
8. Chang CC, Chang CT, Chiang SJ, Liaw BJ, Chen YZ (2010) Oxidative steam reforming of methanol over CuO/ZnO/CeO2/ZrO2/Al2O3 catalysts. Int J Hydrog Energy 38:4397–4406. https://doi.org/10.1016/j.ijhydene.2010.05.066
9. Pinzari F, Patrono P, Costantino U (2006) Methanol reforming reactions over Zn/TiO_2 catalysts. Catal Commun 7:696–700. https://doi.org/10.1016/j.catcom.2006.02.015
10. Pinzari F (2021) The effect of the preparation on the catalytic activity of ZnO/TiO_2 in the methanol steam reforming reaction. Reac Kinet Mech Cat 134:23–35. https://doi.org/10.1007/s11144-021-02044-2
11. Gribovskii AG, Makarshin LL, Andreev DV, Korotaev SV, Dutov PM, Khantakov RM, Reshetnikov SI, Parmon VN (2009) Efficiency of Zn/TiO_2 catalyst operation in a microchannel reactor in methanol steam reforming. Kinet Catal 50:15–21. https://doi.org/10.1134/S0023158409010029
12. Deshmane VG, Owen SL, Abrokwah RY, Kuila D (2015) Mesoporous nanocrystalline TiO_2 supported metal (Cu Co, Ni, Pd, Zn, and Sn) catalysts: effect of metal-support interactions on steam reforming of methanol. J Mol Catal A Chem 408:202–213. https://doi.org/10.1016/j.molcata.2015.07.023
13. Eaimsumang S, Prataksanon P, Pongstabodee S, Luengnaruemitchai A (2020) Effect of acid on the crystalline phase of TiO_2 prepared by hydrothermal treatment and its application in the oxidative steam reforming of methanol. Res Chem Intermed 46:1235–1254. https://doi.org/10.1007/s11164-019-04031-8
14. Xiao J, Mao D, Guo X, Yu J (2015) Methanol synthesis from CO_2 hydrogenation over CuO–ZnO–TiO_2 catalysts: the influence of TiO_2 content. Energy Technol 3:32–39. https://doi.org/10.1002/ente.201402091
15. Xiao J, Mao D, Guo X, Yu J (2015) Effect of TiO_2, ZrO_2, and TiO_2–ZrO_2 on the performance of CuO–ZnO catalyst for CO_2 hydrogenation to methanol. Appl Surf Sci 338:146–153. https://doi.org/10.1016/j.apsusc.2015.02.122
16. Zhang L, Zhang Y, Chen S (2012) Effect of promoter SiO_2, TiO_2 or SiO_2-TiO_2 on the performance of CuO–ZnO–Al_2O_3 catalyst for methanol synthesis from CO2 hydrogenation. Appl Catal A 415–416:118–123. https://doi.org/10.1016/j.apcata.2011.12.013
17. Zhang L, Zhang Y, Chen S (2011) Effect of promoter TiO_2 on the performance of CuO–ZnO–Al_2O_3 catalyst for CO_2 catalytic hydrogenation to methanol. J Fuel Chem Technol 39:912–917. https://doi.org/10.1016/s1872-5813(12)60002-4
18. Khani Y, Tahay P, Bahadoran F, Safari N, Soltanali S, Alavi A (2020) Synergic effect of heat and light on the catalytic reforming of methanol over Cu/x-TiO_2(x=La, Zn, Sm, Ce) nanocatalysts. Appl Catal A 594:117456. https://doi.org/10.1016/j.apcata.2020.117456-117466
19. Andreev DV, Sergeev EE (2021) Methanol steam reforming on Cd–Zn/TiO_2 and Cu–Zn/TiO_2 catalysts in a microchannel reactor. Catal Ind 13:150–160. https://doi.org/10.1134/S2070050421020021
20. Liao S, Donggen H, Yu D, Su Y, Yuan G (2004) Preparation and characterization of ZnO/TiO2, SO42-/ZnO/TiO2 photocatalyst and their photocatalysis. J Photochem Photobiol A 168:7–13. https://doi.org/10.1016/j.jphotochem.2004.05.010
21. Liu Z, Liu C, Ya J, Lei E (2011) Controlled synthesis of ZnO and TiO_2 nanotubes by chemical method and their application in dye-sensitized solar cells. Renew Energy 36:1177–1181. https://doi.org/10.1016/j.renene.2010.09.019
22. Chen X, Chen Y, Yang H, Wang X, Che Q, Chen W, Chen H (2019) Catalytic fast pyrolysis of biomass: selective deoxygenation to balance the quality and yield of bio-oil. Bioresour Technol 273:153–158. https://doi.org/10.1016/j.biortech.2018.11.008

23. Makawana JA, Sangani CB, Yao YF, Duan YT, Lv PC, Zhu HL (2016) Recent developments of metal and metal oxide nanocatalysts in organic synthesis. Mini Rev Med Chem 16:1303–1320. https://doi.org/10.2174/1389557516666160823143243
24. Danish MSS, Estrella LL, Alemaida IMA, Lisin A, Moiseev N, Ahmadi M, Nazari M, Wali M, Zaheb H, Senjyu T (2021) Photocatalytic applications of metal oxides for sustainable environmental remediation. Metals 11(80):1–25. https://doi.org/10.3390/met11010080
25. Zarzuela R, Almoraima Gil ML, Carretero J, Carbú M, Cantoral JM, Mosquera MJ (2021) Development of a novel engineered stone containing a CuO/SiO_2 nanocomposite matrix with biocidal properties. Constr Build Mater 303:124459. https://doi.org/10.1016/j.conbuildmat.2021.124459
26. Kakakhel MA, Wu F, Gu JD, Feng H, Shah K (2019) Controlling biodeterioration of cultural heritage objects with biocides: a review. Int Biodeterior Biodegrad 143:10472. https://doi.org/10.1016/j.ibiod.2019.104721
27. Okamoto Y, Fukino K, Imanaka T, Teranishi S (1983) Surface characterization of CuO-ZnO methanol-synthesis catalysts by X-ray photoelectron spectroscopy. 1. Precursor and calcined catalysts. J Phys Chem 87:3740–3747. https://doi.org/10.1021/j100242a034
28. Zheng JH, Jiang Q, Lian JS (2011) Synthesis and optical properties of flower-like ZnO nanorods by thermal evaporation method. Appl Surf Sci 257:5083–5087. https://doi.org/10.1016/j.apsusc.2011.01.025
29. Reyes-Coronado D, Rodríguez-Gattorno G, Espinosa-Pesqueira ME, Cab C, de Coss R, Oskam G (2008) Phase-pure TiO_2 nanoparticles: anatase, brookite and rutile. Nanotechnology 19:145605. https://doi.org/10.1088/0957-4484/19/14/145605
30. Akgul FA, Akgul G, Yildirim N, Unalan HE, Turan R (2014) Influence of thermal annealing on microstructural, morphological, optical properties and surface electronic structure of copper oxide thin films. Mater Chem Phys 147:987–995. https://doi.org/10.1016/j.matchemphys.2014.06.047
31. Yin M, Wu CK, Lou Y, Burda C, Koberstein JT, Zhu Y, O'Brien S (2005) Copper oxide nanocrystals. J Am Chem Soc 127:9506–9511. https://doi.org/10.1021/ja050006u
32. Hu T, Yin H, Zhang R, Wu H, Jiang T, Wada Y (2007) Gas phase hydrogenation of maleic anhydride to γ-butyrolactone by Cu–Zn–Ti catalysts. Catal Commun 8:193–199. https://doi.org/10.1016/j.catcom.2006.06.009
33. Velu S, Suzuki K, Kapoor M, Ohashi F, Osaki T (2001) Selective production of hydrogen for fuel cells via oxdative steam reforming of methanol over CuZnAl(Zr)-oxide catalysts. App Catal A 213:47–63